A Tapered Slot Rectangular Ultra-wideband Microstrip Patch Antenna for Radio Frequency Energy Harvesting

P. S. Chindhi, H. P. Rajani, and G. B. Kalkhambkar

Abstract A tapered slot rectangular microstrip ultra-wideband (UWB) patch antenna is proposed in this chapter for radio frequency (RF) energy harvesting. The RF energy harvesting technologies are intensifying steadily because of constraints in energy storage and wired power supply. Hence, harvesting energy from RF sources is a promising technique for fulfilling the inimitable power prerequisites for powering smart sensors. Here, to achieve ultra-wideband, a rectangular structure is modified in a tapered slot. The antenna structure is optimized and simulated by using electromagnetic high-frequency structural simulator (HFSS) software, and the measured bandwidth defined by return loss <-10 dB is from 3.76 to 19.52 GHz with <2 voltage wave standing ratio (VSWR) throughout the band.

Keywords Radio frequency · Return loss · Wideband · Tapered slot · Notch

1 Introduction

As the demand for power is growing, the need for alternative energy sources has become essential; at the same time, the RF power density is increasing since there is an increase in frequency bands such as WLAN, GSM, DCS, 3G, 4G LTE, and 5G. Self-powered electronic devices have gained momentous attention in a wide range of applications such as permanently inserted sensors inside the human body,

P. S. Chindhi (✉)
Department of Electrical Engineering, Sant Gajanan Maharaj College of Engineering, Mahagaon, India

P. S. Chindhi · G. B. Kalkhambkar
Shivaji University Kolhapur, Kolhapur, India

H. P. Rajani
Department of Electronics and Communication Engineering, KLE's Dr. MSSCT, Visvesvaraya Technological University, Belagavi, India

G. B. Kalkhambkar
Department of Electronics and Telecommunication Engineering, Sant Gajanan Maharaj College of Engineering Mahagaon, Mahagaon, India

A. Sivasubramanian et al. (eds.), *Futuristic Communication and Network Technologies*, Lecture Notes in Electrical Engineering 792,
https://doi.org/10.1007/978-981-16-4625-6_36

Table1 Incremental development of RF energy sources in India

Years	Number of mobile towers in lakh	Number of mobile subscribers in million	Number of base transceiver stations (BTS) (^as on 12.07.2019)
2017	412,387	1170.59	1384737
2018	–	1188.99	2035488
2019	560162^	1161.71	2180224^

building walls, and textile wearable antenna. The RF energy harvesting technology is expected to rise with the Internet of Things (IoT). According to Gartner, in a few years, there will be 25 billion perpetually connected things and some year's later, 10 trillion connected sensors [1–3]. Devices that work within the limits of harvesting capability are Bluetooth transceiver, wireless sensor/hearing aid, remote sensors, RFID tags, watches/calculators, and processor clock [4]. According to the Economics Research Unit, Department of Telecommunications Ministry of Communications, Government of India, New Delhi, 2019, Table 1 indicates the growth in the RF energy surrounding us [5]. A triple-band differential antenna and reflector plate with a spacing of 28 mm are presented; the overall size of the rectenna is higher [6]. In Ref. [7], for higher bandwidth, CPW-feed fractal antenna is simulated and tested' to achieve higher bandwidth, slotted equilateral triangles are introduced in the CPW-feed circular patch. In Ref. [8], the E-shaped patch antenna with two parallel slots and the partial ground is incorporated to enhance the bandwidth. At 936 MHz, the current distribution density around the slot1, slot2, and at the edge of the slot is uniform. Circularly polarized shorted square-ring slot antenna for the GSM 900 band is presented in Ref. [9]. The circular patch antenna and parametric study on various parameters are taken into consideration to enhance the bandwidth of the antenna [10]. A multilayer stacked antenna loaded with an octagon radiator with tapered slits and an unequal slotted circular patch improves the bandwidth and polarization characteristics [11]. The various methods to enhance bandwidth are compressively reviewed in [12]. Different impedance matching techniques that are important to build an efficient energy harvesting circuit are studied in Ref. [13]. The hexagonal fractal antenna helps in improving bandwidth [14].

In the planned work, UWB rectangular microstrip patch antenna with a tapered slot is simulated in HFSS software, which is useful for the RF energy harvesting. The impact of stepwise change in the radius on the bandwidth and gain of an antenna is observed. In the first iteration, with an increase in the radius of the circular slot, the bandwidth is degraded; whereas in the second iteration where we decreased the radius of the circular slot, it is observed that the bandwidth is improved, but the gain is not satisfactory. To compensate for the loss in the gain, a notch is inserted at the periphery of the circular slot. The parametric study of the notch dimension is performed to arrive at good impedance matching. A good combination of circular slot and the notch gave the enhanced bandwidth and positive gain which make this antenna a good candidate for RF energy harvesting. The comparison of Ref. [6–11]

in terms of overall dimensions and bandwidth with the proposed geometry is given in Table 7. The detail conceptual block diagram of a RF power harvesting system is presented in [15].

The chapter is organized as follows: Sects. 2 and 3 describe the antenna design and its parametric study and observations, respectively. Section 4 depicts results and discussion along with a comparison of other related works. Section 5 describes the conclusion, and in Sect. 6, future scope is specified.

2 Antenna Design

The proposed UWB rectangular microstrip patch antenna with a tapered slot is shown in Fig. 1. A low-cost double-sided printed circuit board (PCB) of flame retardant-4 (FR4) substrate with a thickness of 1.5 mm, dielectric constant 4.4, and loss tangent (tanδ) 0.02 is selected. The patch length and width are 110 mm and 80 mm, respectively. The detailed design parameters of the proposed antenna are given in Table 2

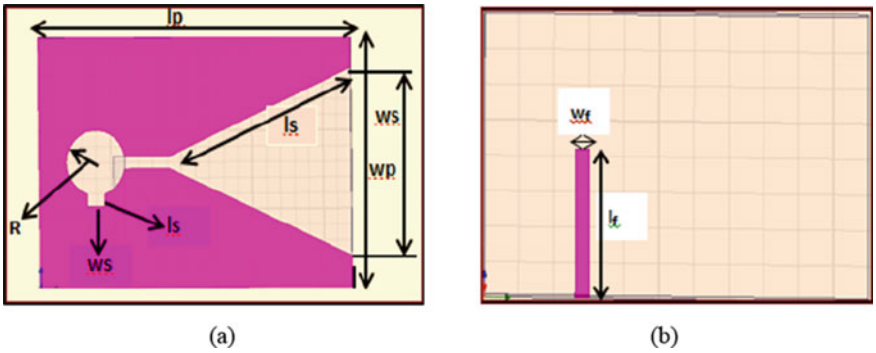

Fig. 1 Proposed UWB microstrip antenna. **a** Top view. **b** Bottom view

Table 2 The specification of the design parameters

S. No.	Parameters	Value
1	Design frequency (f_r)	5 GHz
2	Dielectric constant (ε_r)	4.4
3	Height of the substrate (h)	1.5 mm
4	Loss tangent (tanδ)	0.02
5	Width of the patch (w_p)	80 mm
6	Length of the patch (l_p)	110 mm
7	Width of the ground (w_p)	4 mm
8	Length of the ground (L_p)	42 mm

3 Parametric Study and Observations

1. **Setp#1 Increase in radius of circular slot without notch.**

In the initial iteration, a circular slot with a radius $R_1 = 12$ mm is made; the bandwidth of 4.52 GHz is obtained. In the subsequent iterations, radius of the circular slot is increased with 2 mm. At $R_5 = 12.8$ mm, the bandwidth is reduced from 4.52 to 2.95 GHz. The various antenna parameters with an increasing radius of the circular slot are tabulated in Table 3. The return loss versus frequency plot is shown in Figs. 2 and 3.

2. **Step#2 Decrease in radius of circular slot without notch**

In the next iterations, the radius of the circular slot is decreased from $R_1 = 12$ mm to $R_6 = 11.8$ mm; the bandwidth is increased from 4.52 to 4.62 GHZ. In the next iteration, the radius of the circular slot is decreased at the steps of 2 mm. By decreasing the radius of the circular slot, there is a steady increase in the bandwidth from 4.52 to 4.93 GHz. The various antenna parameters with a decrease in the radius of the circular slot are tabulated in Table 4. The return loss versus frequency plot is shown in Fig. 4.

Table 3 Antenna performance comparison at R_1, R_2, R_3, R_4, and R_5 without notch

Variable parameter (mm)	Resonant frequency (GHz)	Return loss (dB)	Peak directivity	Peak gain (dBi)	Bandwidth (GHz)
$R_1 = 12.0$	4.54	−27.83	0.89	0.76	4.52
$R_2 = 12.2$	4.54	−34.77	0.93	0.97	4.53
$R_3 = 12.4$	4.72	−31.61	0.91	0.78	4.55
$R_4 = 12.6$	5.00	−32.80	0.88	0.75	4.55
$\boldsymbol{R_5 = 12.8}$	5.18	−41.35	0.82	0.70	2.95

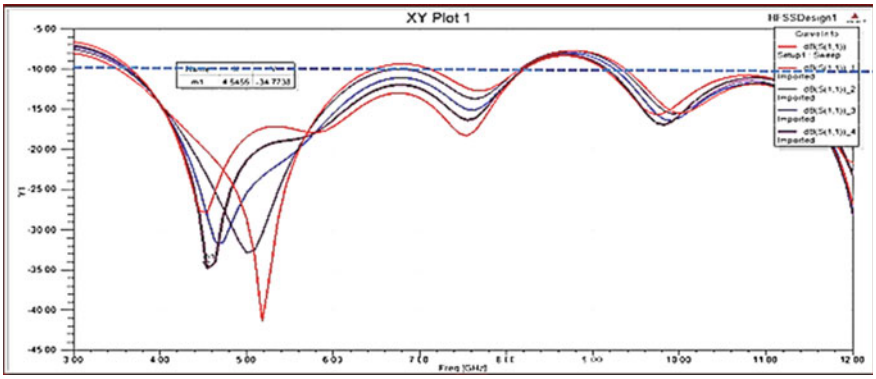

Fig. 2 Graph of the return loss versus frequency without notch at R_1, R_2, R_3, R_4, and R_5

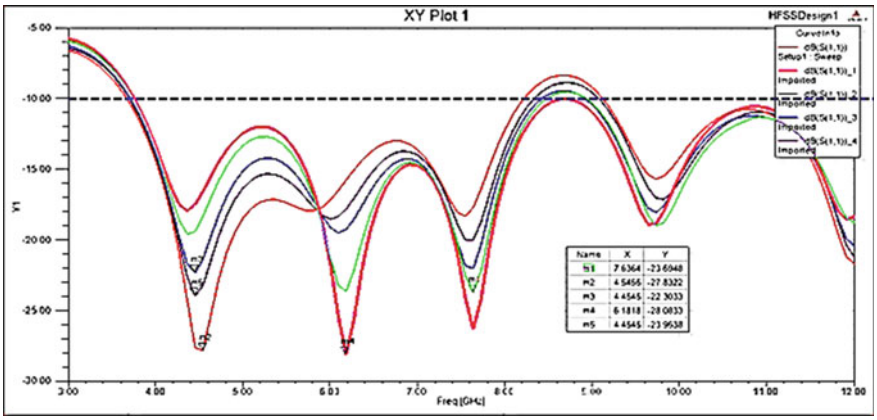

Fig. 3 Graph of the return loss versus frequency without notch at R_1, R_{10}, R_{11}, R_{12}, R_{13} and R_{14}

Table 4 Antenna performance comparison at R_1, R_6, R_7, R_8, and R_9 without notch

Variable parameter (mm)	Resonant frequency (GHz)	Return loss (dB)	Peak directivity	Peak gain (dBi)	Bandwidth (GHz)
$R_1 = 12.0$	4.54	−27.83	0.89	0.76	4.52
$R_6 = 11.8$	4.45	−23.95	0.95	0.80	4.62
$R_7 = 11.6$	4.45	−22.30	0.98	0.83	4.70
$R_8 = 11.4$	7.63	−23.69	0.94	0.78	4.73
$\boldsymbol{R_9 = 11.2}$	6.18	−28.08	0.96	0.80	4.93

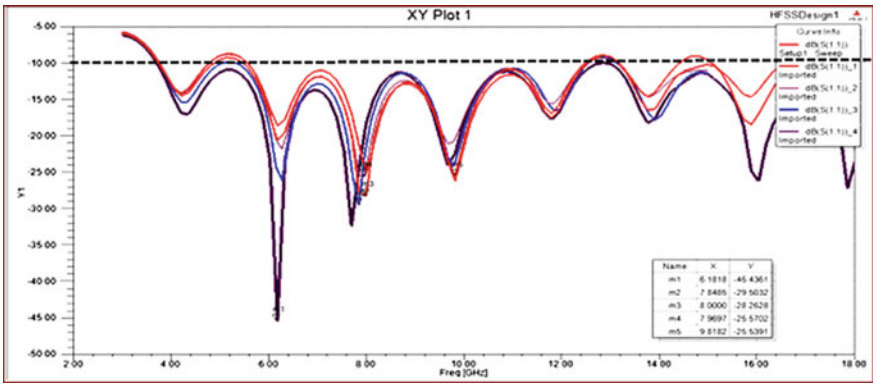

Fig. 4 Graph of the return loss versus frequency without notch at R_{10}, R_{11}, R_{12}, R_{13}, and R_{14}

3. **Step#3 Decrease in radius of circular slot without notch**
   As in step #2, there is a gradual increase in the bandwidth, so to get higher bandwidth in step #3, the radius of the circular slot is decreased by 10 that is 12–10 mm and in subsequent iterations, it decreased at a step of 2 mm. At R_{10} = 10 mm, the band width is 6.90 GHz, and at R_{14} = 10.8 mm, the bandwidth is 9.07 GHz. In Table 5, the bandwidth and other antenna parameters are tabulated with a decrease in the radius of the circular slot; Fig. 5 shows the return loss versus frequency plot for R_{10} to R_{14}.

4. **Step#4 Decrease in radius of circular slot with notch**

In step#4, the radius of the circular slot is maintained constant as in step#3, and a notch is inserted at the lower side of the circular slot as shown in Fig. 1. When the radius of the circular slot is 10 mm (R_{15}) with a notch, the bandwidth is 13.96 GHz, but at R16, R18 and R19, there is a decrease in bandwidth. At R = 17 and radius R = 10.4 with a notch, the bandwidth is 15.74 GHz. The parametric variation in the antenna results at R = 15 to R=19 is tabulated in Table 6. Fig. 6 shows the return loss versus frequency plot for R_{15} to R_{19}. In Fig. 6, green color indicates the higher

Table 5 Antenna performance comparison at R_{10}, R_{11}, R_{12}, R_{13}, and R_{14} without notch

Variable parameter (mm)	Resonant frequency (GHz)	Return loss (dB)	Peak directivity	Peak gain (dBi)	Bandwidth (GHz)
R_{10} = 10.0	9.81	−25.53	1.03	0.85	6.90
R_{11} = 10.2	8.00	−28.26	1.03	0.84	8.75
R_{12} = 10.4	7.96	−25.57	0.97	0.79	8.73
R_{13} = 10.6	7.84	−29.50	1.00	0.82	8.77
R_{14} = 10.8	6.18	−45.43	1.03	0.85	9.07

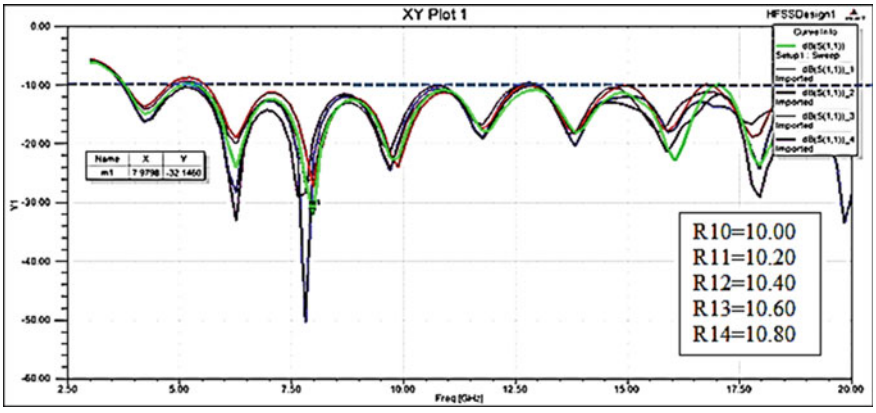

Fig. 5 Graph of the return loss versus frequency with notch at R_{15}, R_{16}, R_{17}, R_{18}, and R_{19}

Table 6 Antenna performance comparison at R_{15}, R_{16}, R_{17}, R_{18}, and R_{19} with notch

Variable parameter (mm)	Resonant frequency (GHz)	Return loss (dB)	Peak directivity	Peak gain (dBi)	Bandwidth (GHz)
$R_{15} = 10.0$	7.97	−27.34	1.01	0.82	13.96
$R_{16} = 10.2$	7.80	−26.84	1.00	0.82	7.03
$R_{17} = 10.4$	*7.97*	*−32.16*	*0.99*	*0.82*	*15.74*
$R_{18} = 10.6$	7.80	−50.24	1.01	0.83	7.29
$R_{19} = 10.8$	6.26	−33.14	0.96	0.78	7.03

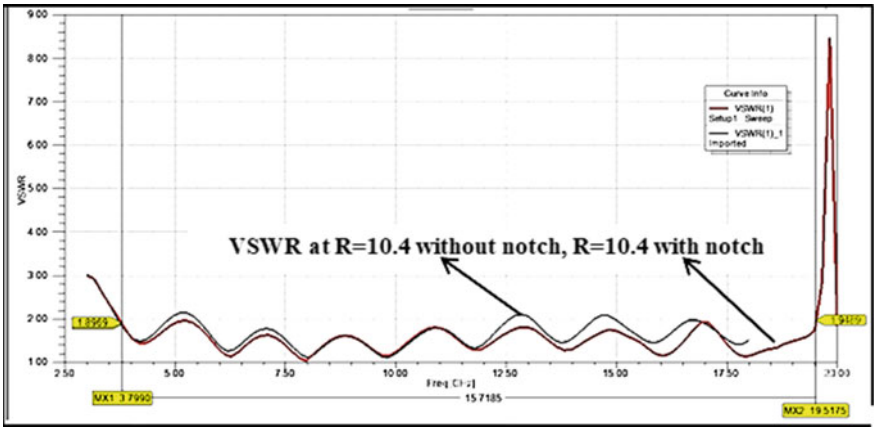

Fig. 6 Simulated VSWR of the proposed antenna with and without notch at $R = 10.4$

bandwidth; the range of bandwidth is 3.76–19.52 GHz. Fig. 7 shows the simulated VSWR of the proposed antenna with and without a notch at $R = 10.4$. The VSWR is <2 throughout the band. The VSWR at $R = 10.4$ mm without notch is slightly high, and at $R = 10.4$ with notch, the VSWR is within the standard value (<2).

4 Results and Discussion

In Fig. 7, the current distribution at 5 GHz is shown for the radius $R = 12$ mm (Fig. 7c), for $R = 10$ mm (Fig. 7d), for $R = 10.2$ mm with notch (Fig. 7e), and for $R = 10.4$ mm with notch (Fig. 7f). In the final iteration, the bandwidth is increased ranging from 3.76 to 19.52 GHz due to improved current distribution.

The proposed antenna performance is compared with the recent literature; it is observed that the present work shows the ultra-wideband performance which is suitable for the RF energy harvesting in the band ranging from 3.76 to 19.52 GHz.

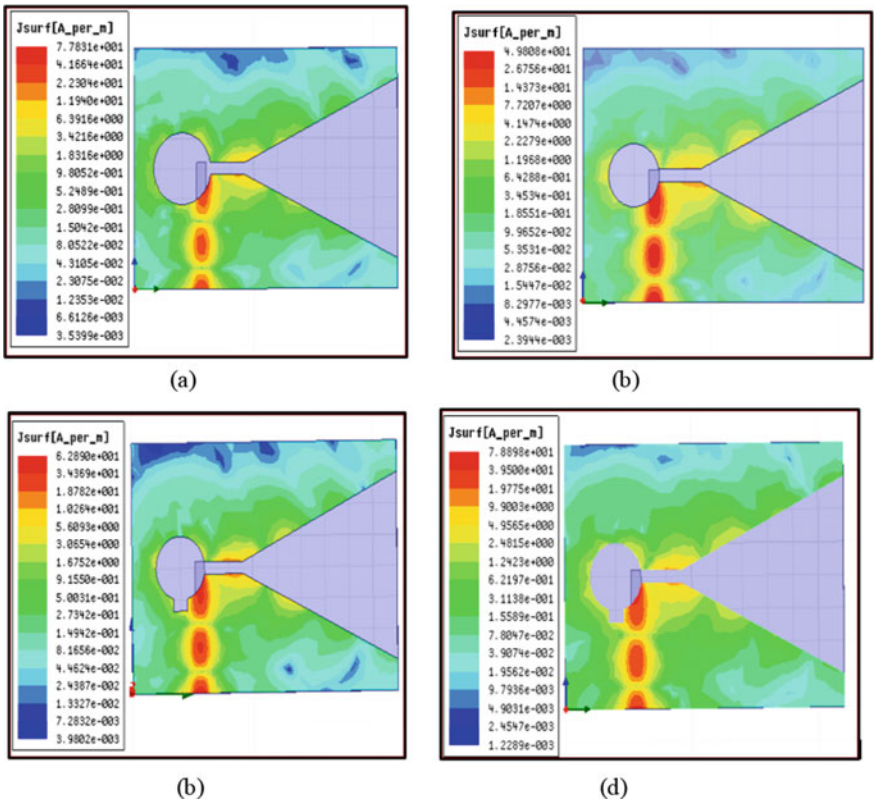

Fig. 7 Current distribution. **a** At $R = 12.00$ mm without notch. **b** At $R = 10.00$ mm without notch. **c** At $R = 10.2$ mm with notch. **d** At $R = 10.4$ mm with notch

Compared to the literature mentioned in Table 7 which works in the specific bands only, the proposed antenna is a better candidate in terms of bandwidth as well as size.

Table 7 Comparison of other related works

Sr. No	References	Frequency (GHz)	Size (mm^2)
1	Devi et al. [8]	GSM 900 band	106 × 89
2	Ghosh [9]	GSM 900 band	140 × 140
3	Agrawal et al. [10]	0.89–5.53 GHz	120 × 100
4	Chandravanshi et al. [6]	2.1 GHz, 2.4–2.48 GHz, 3.3–3.8 GHz	120 × 120
5	Bai et al. [7]	0.88–8.45 GHz	100 × 100
6	Jie et al. [11]	0.908–0.922 GHz, 2.35–2.50 GHz	120 × 120
7	Proposed work	3.76–19.52 GHz	110 × 80

5 Governing Equations for RF Energy Harvesting

Figure 8 shows the conceptual representation of RF energy harvesting, which consists of a transmission antenna and receiving antenna with a power management circuit. The received power is calculated by the Friis transmission equation (FTE),

$$P_{\mathrm{R}} = \frac{P_{\mathrm{T}} G_{\mathrm{T}} G_{\mathrm{R}} \lambda^2}{(4\pi R)^2} \tag{1}$$

where

P_{R} is power at the receiver antenna.

G_{R} is receiver antenna gain relative to the isotropic source (dBi).

λ is the wavelength of the electromagnetic signal, which is equal to the speed of light in vacuum divided by the signal frequency $= c/f$.

The loss of power in space can be characterized by free-space path loss (FSPL), which is the loss of signal power during propagation in free space. Calculating FSPL requires information about the antenna gain, frequency of transmitting wave, and distance between the transmitter and receiver. The FSPL for far field is,

$$P_{\mathrm{L}} = \frac{P_{\mathrm{T}}}{P_{\mathrm{R}}} = \frac{(4\pi R)^2}{G_{\mathrm{T}} G_{\mathrm{R}} \lambda^2} = \frac{(4\pi f R)^2}{G_{\mathrm{T}} G_{\mathrm{R}} c^2} = \frac{4}{G_{\mathrm{T}} G_{\mathrm{R}}} (kR)^2 \tag{2}$$

$$P_{\mathrm{L}}(\mathrm{dB}) = 20\log_{10}(f) + 20\log_{10}(R) + 20\log_{10}\left(\frac{4\pi}{c}\right) - G_{\mathrm{T}} - G_{\mathrm{R}} \tag{3}$$

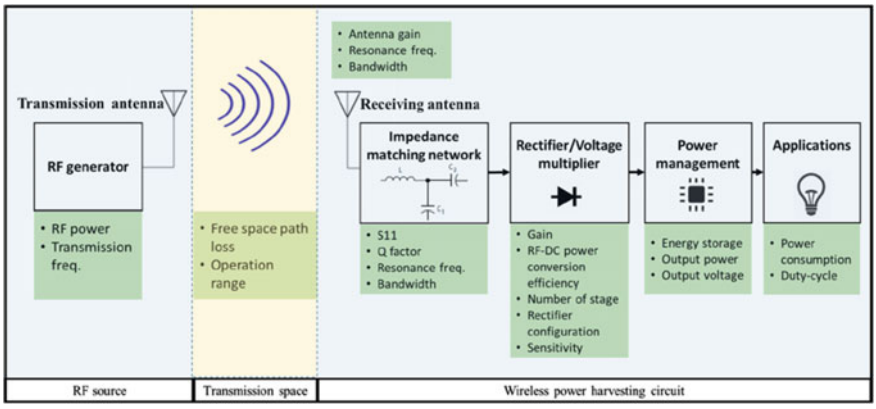

Fig. 8 Conceptual representation of RF energy harvesting system, Ref. [15]

In case f is measured in MHz, distance R is measured in km, and gain G_T and G_R are measured in dBi, the above function becomes

$$P_L(\text{dB}) = 20\log_{10}(f) + 20\log_{10}(R) + 32.44 - G_T - G_R \quad (4)$$

6 Conclusion

The bandwidth of the proposed tapered slot UWB rectangular microstrip patch antenna was enhanced by the optimization of circular slot dimensions. At initial iteration $R = 10$ mm without notch, the frequency band of the antenna lies between 5.57 and 6.89 GHz. At final iteration, the frequency band of the proposed rectangular tapered slot microstrip patch antenna with notch length 4.04 mm and width 6 mm antenna bandwidth lies between 3.76 and 19.52 GHz. The VSWR is <2 throughout the band. This antenna has a wide bandwidth, so it is suitable for RF energy harvesting and WLAN applications.

7 Future Work

The work given in this chapter shows the trade-off between bandwidth and gain due to inverse relationship between bandwidth and quality factor $Q = 1/\text{B.W}$, further attempts can be extended for improving the gain by using metamaterials, slits, parasitic patch, differential patches, folded ground, vertical embedded ground plane, etc.

References

1. Gartner (2015) Predicts 2015: the internet of things
2. Lim EG et al (2014) Compact size of textile wearable antenna. In: Proceedings of the international multi configuration of engineering and computer science (IMECS), vol 2
3. Shawalil S et al (2019) 2.45 GHz wearable rectenna array design for microwave energy harvesting. Ind J Electr Eng Comput Sci 14(2)
4. Charalampidisa G, Papadakisb A, Samarakoua M (2019) Power estimation of RF energy harvesters 157:892–900. https://doi.org/10.1016/j.egypro.2018.11.255
5. Telecom Statist India (2019) Economics Research Unit Department of Telecommunications Ministry of Communications Government of India, New Delhi
6. Chandravanshi S, Akhtar MA (2018) Design of triple band differential rectenna for RF energy harvesting. IEEE Trans Antennas Propagt 66(6). https://doi.org/10.1109/TAP.2018.2819699
7. Bai X, Zhang J-w, Xu L-j, Zhao B-h (2018) A broadband CPW fractal antenna for RF energy harvesting. Aces J 33(5):1054–4887 © ACES
8. Devi KKA et al (2012) Design of a wideband 377Ω E-shaped patch antenna for RF energy harvesting. Microwave Opt Technol Lett 54(3)

9. Ghosh S (2016) Design and testing of rectifying antenna for RF energy scavenging in GSM 900 band, 36–44, received 28 Jan 2016, Accepted 30 Oct 2016, published online: 23 Nov 2016. https://doi.org/10.1080/1206212X.2016.1259801
10. Agrawal S, Parihar MS, Kondekar PN (2017) Broadband Rectenna for radio frequency energy harvesting application, pp 347–353, published online: 29 Aug 2017. https://doi.org/10.1080/03772063.2017.1356755
11. Jie AM et al (2019) A dual-band efficient circularly polarized rectenna for RF energy harvesting systems. Int J RF Microw Comput Aided Eng 29: e21665
12. Geeta K, Rajashri K, Pradeep C (2018) A survey on microstrip patch antenna parameters enhancement techniques: a progress in last decade. JASC J Appl Sci Computat 5(7). ISSN NO: 0076-5131
13. Chindhi PS, Rajani HP, Kalkhambkar GB (2018) A review on radio frequency [RF] energy harvesting systems. JASC J Appl Sci Computat 5(8). ISSN NO: 1076-5131
14. Geeta K, Khanai RN, Chindhi P, Fractals: a novel method in the miniaturization of a patch antenna with bandwidth improvement. In: Information and communication technology for intelligent systems, pp 629–63. https://doi.org/10.1007/978-981-13-1742-2_63
15. Tran L, Cha H, Park W (2017) RF power harvesting: a review on designing methodologies and applications. Micro and Nano Syst Lett 5:14. https://doi.org/10.1186/s40486-017-0051-0